JOURNAL OF Applied Polymer SCIENCE

Morphology, Polymorphism, and Metal Ion Adsorption Studies of Electrospun Nanofibers Based on PVDF and Organically Modified Layered Double Hydroxide

Mallinath S. Birajdar,* Santosh D. Wanjale,† Sunil P. Lonkar

Polymer Science and Engineering Division, National Chemical Laboratory, Dr. Homi Bhabha Road, Pashan, Pune 411008, Maharashtra, India

*Present address: Department of Chemical Engineering and Material, Science, Chung-Ang University, 221 Heukseok-dong, Dongiak-gu, Seoul 15-756, South Korea.

†Present address: Aditya Birla Science and Technology Company Ltd., Tal. Panvel, Dist. Raigad 410208, Maharashtra, India.

Correspondence to: S. D. Wanjale (E-mail: santosh.wanjale@adityabirla.com)

ABSTRACT: Nonwoven nanofiber mats of polyvinylidene fluoride (PVDF) with modified layered double hydroxide (MLDH) were prepared by electrospinning. The fiber morphology was studied using scanning electron microscopy. X-ray diffraction and FTIR spectroscopy was used to characterize the polymorphism in electrospun mats. Fibers of diameter in the range 80–800 nm with beads of about 2–3 μm size were observed for pure PVDF, while in case of PVDF/MLDH nanocomposites the number and size of beads were found to be significantly reduced. Uniform and fine nanofibers were obtained at lower content of MLDH, but slightly rough surface was seen for higher content. FTIR and X-ray diffraction patterns signify various crystalline forms of electrospun PVDF. The content of polar β-crystalline phase of PVDF, which exhibit piezo and ferroelectric properties was found to be enhanced significantly due to reinforcement of MLDH. Use of these nanofiber mats for heavy metal Cu (II) removal was explored. © 2013 Wiley Periodicals, Inc. J. Appl. Polym. Sci. 000: 000–000, 2013

KEYWORDS: adsorption; electrospinning; fibers

Received 16 April 2013; accepted 26 June 2013; Published online 00 Month 2013

DOI: 10.1002/app.39729

INTRODUCTION

Polyvinylidene fluoride (PVDF) is an important polymer because of its polymorphism which exhibits piezo, pyro, and ferroelectric properties. This partially fluorinated polymer is one of the most interesting and promising materials for a broad range of applications such as nonlinear optics, piezoelectric, and pyroelectric materials, and microwave transducers, dye-sensitized solar cells as a solid polymer electrolyte, biomedical fields, and ultrafiltration membranes. Three main crystal architectures (α, β, and γ) are obtained under ordinary crystallization conditions.[1–4] The most common phase, called α, has a monoclinic unit cell with a TGT$\bar{G}$ chain conformation.[2,3] The β phase has an orthorhombic unit cell, with the chains in an all trans conformation.[1] The γ form has an orthorhombic unit cell with T_3 GT_3 $\bar{G}$ chain conformation.[2,3]

PVDF shows five different crystalline structures, such as α, β, γ, δ, and ε.[5] The β crystalline (hexagonal crystalline structure) form exhibits piezoelectric, ferroelectric, and pyroelectric properties.[6] various techniques have been reported to obtain a β crystalline form. These include, uni-axial stretching of α crystalline film at high temperatures, epitaxial growth with lattice matching, and melt crystallization at high pressure. In previous study,[7] it is demonstrated that organically modified clay induces β crystalline form in PVDF by melt compounding. Tashiro et al.[8] synthesized PVDF/organically modified layered titanate nanocomposite by melt intercalation technique and showed that the neat PVDF predominantly formed α phase in the crystallization temperature range of 110–150°C. The nanocomposite exhibited mainly α form along with presence of β and γ forms at crystallization temperature ranges from 110 to 135°C. Interestingly, at 140–150°C significant amount of γ and β form coexisted with slight amount of α form. PVDF can also be crystallized into the β crystalline form from organic solvents such as dimethyl formamide if the solution casting is carried at below 70°C.[9]

Electrospinning is an important and efficient method to prepare submicron to nanoscale fibers and it is a simple technique to obtain a β crystalline form of PVDF from solution. Electrospinning of PVDF with ferrite nanoparticles revealed that the amount of ferroelectric β phase, and γ phase was increased with the content of ferrite nanoparticles.[10] Han et al.[11] demonstrated

that polymorphism in PVDF can be controlled through electrospinning. They showed that the various crystal forms of PVDF like α, β, and γ phase could be fabricated by controlling the electrospinning parameters such as, solvent, electrospinning temperature, feed rate, and collector to needle tip distance. Recently, Cebe et al.[12] investigated the morphology and crystal polymorphism of electrospun nanofibers prepared using PVDF with Lucentite clays (modified and unmodified) and showed that the clays induced more extended PVDF conformers, characteristic of β and γ phases with low amount of α phase conformers.

To the knowledge of the authors, few papers were published on this subject[12,13] in which formation of β phase was ascribed to a peculiar interaction between electrospinning which favors orientation of the chains, and clay which hinders polymer motion.

Various types of layered double hydroxides (LDH) are being used in polymer nanocomposite as nanofiller because of the layered structure that is expandable with different kind of surfactants, its anion exchange capacity and its flame retardant properties.[14] Organically modified LDH (MLDH) finds applications in the areas of catalysis, photochemistry and electrochemistry. These materials are also of relevance to adsorption, separation, and membrane technologies.[15] Effluents of waste water contain pollutants of positively and negatively charged particles. It is known that LDH have high ion exchange capacity, large surface area, and regeneration ability, so that these could be used as adsorbents to remove these particles from wastewater.[16] In this article, we present the use of the electrospinning technique to study the effect of LDH on the development of crystalline phases in PVDF and nonwoven mats for metal adsorption studies.

EXPERIMENTAL

Materials

PVDF (Solef) with molecular weight of 1×10^5 g/mol was purchased from Solvay, Belgium. Dimethylformamide (Merck, India), acetone (Merck, India), $MgCl_2{\cdot}6H_2O$ (Aldrich), $AlCl_3{\cdot}6H_2O$ (Aldrich), NaOH (Spectrochem, India), and sodium dodecyl sulfate (DDS) (>98% $CH_3(CH_2)_{11}O\ SO_3Na$, Spectrochem, India) were used as received without further purification.

Hydrotalcite-type material Mg_2Al–LDH was prepared by simultaneously adding drop wise an aqueous solution of sodium hydroxide (2.0 M) and a mixed aqueous solution of magnesium chloride and aluminum chloride (total metal concentration of 1 M with a Mg^{2+}/Al^{3+} molar ratio of 2.0) into a large plastic beaker containing 100-mL de-ionized water which had been boiled and stored under nitrogen before use. Nitrogen was bubbled throughout the process to minimize dissolved carbonate. During the reaction, temperature and pH of the reaction mixture were maintained at 25 ± 1°C and 10 ± 0.2, respectively. The suspension was stirred for 3 h, transferred to plastic bottles, and placed in an oven at 65°C for 4 days. After cooling to room temperature, the suspension was centrifuged and the precipitate washed extensively using de-ionized water until free of chloride ($AgNO_3$ test). The product was dried at 65°C and finely ground.

Pristine LDH is practically not suitable to prepare polymer nanocomposite due to the very small interlayer distance between two platelets. Because of which intercalation of polymer chains is very difficult; therefore, the pretreatment of LDH is necessary. It has been reported that the compatibility between DMF and LDH had increased due to intercalation of DDS ions, which also helped in improving the dispersion of LDH in DMF.

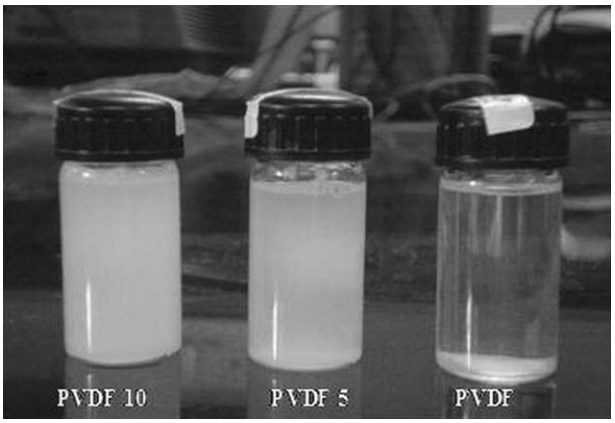

Figure 1. MLDH dispersion in DMF/acetone solvent mixture.

Therefore, organo-modification was carried out by anion exchange reaction. In this experiment, DDS was introduced into the LDH interlayer at a pH value of 6.5 and at a DDS: LDH ratio of 12 mmol g^{-1}. The mixture of LDH and water (1 g/20 mL) was homogenized by stirring before adding the DDS solution. The suspension was stirred at room temperature for 3 days under nitrogen and vigorous stirring. The resulting powder was washed several times with a mixture $EtOH/H_2O$ (50/50), and then dried under vacuum. The pristine Mg_2Al-Cl and DDS modified LDH (MLDH) were characterized by X-ray diffraction and FTIR.

ELECTROSPINNING

The 20 wt % solution of PVDF was prepared in dimethyl formamide (DMF)/acetone solvent mixture of 4 : 1 ratio at 60°C. MLDH was dispersed in a calculated amount of DMF under ultrasonication for about 2 h, and then PVDF/MLDH composite solution was prepared by adding PVDF to the MLDH dispersion. Three compositions, PVDF+0% MLDH, PVDF+5%MLDH, and PVDF+10% MLDH were prepared and labeled as PVDF, PVDF 5, and PVDF 10, respectively. These PVDF/MLDH suspensions were kept for ultrasonication for about 2 h. Figure 1 shows the dispersion of MLDH in PVDF solution. The suspensions were placed in a 10-mL syringe with a needle having an internal diameter of 0.8 mm. A Sage syringe pump was used to feed the suspensions from the syringe to the tip of the needle. A sheet of aluminum foil, connected to the ground was acting as a collector. Electrospinning was carried out at room temperature; the voltage was kept 15 kV and the needle tip to collector distance was 15 cm.

Characterization

SEM. Scanning electron microscopy, [EDAX, Micro Analysis System and Model Phoenix] was used to evaluate the morphology of the electrospun nanofibers. A small portion of aluminum foil on which the nanofiber mat collected was cut and carefully

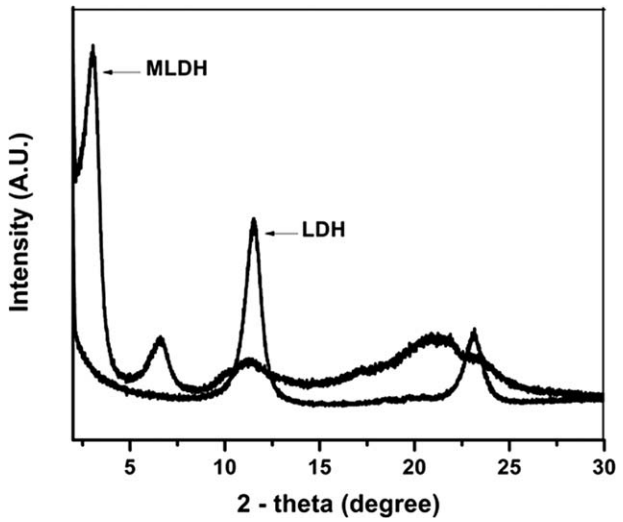

Figure 2. X-ray diffraction pattern for LDH and MLDH.

mounted on the stub to view under the SEM. The mounted stubs were sputtered with gold using a Coating Unit E5000, Polaron Equipment. The images of the micrographs of the fibers were obtained at 5K (5× 1000) and 10K (10× 1000) magnification. The average diameter of the fibers was determined from the SEM images.

XRD. The wide angle X-ray diffraction (WAXD) was carried out using Rigaku X-ray diffractometer (model Dmax 2500) with Cu K_α radiation of $\lambda = 0.154$ nm, operated at 40 kV and 100 mA in the 2-theta range of 2–35°.

FTIR. The functional characteristics of the electrospun nanofibers PVDF and PVDF/MLDH nanofibers were recorded using Fourier Transform infrared spectrometer [Perkin Elmer, spectrometer I]. The recording of spectrum was done in the wavelength range from 4000 to 650 cm^{-1} with a resolution of 4 cm^{-1}. Each spectrum was composed of an average of 40 scans.

DRS. The dielectric analysis was carried out using a high-frequency dielectric spectrometer (3 μHz to 20 MHz) with an Alpha-A high-performance frequency analyzer having a ZGS-BDCS 41201 active sample cell (both Novocontrol Technologies, Hundsangen, Germany). Two disposable gold-plated electrodes of 10 mm diameter and 2 mm thickness were used for the analysis. The dielectric loss of the PVDF and electrospun mats was determined at room temperature.

RESULTS AND DISCUSSION

Characterization of Organically Modified Double Hydroxide

The X-ray diffraction pattern for LDH and MLDH was shown in Figure 2. The figure depicts that these materials are highly crystalline in nature. The basal peak (d_{003}), the interlayer spacing between two metal hydroxide sheets was found to be at 2 theta of 11.51°, whereas the basal position peak for MLDH was found to be at 2 theta of 3.06°. The shift in d_{003} to the lower angle suggests an increase in d-spacing due to intercalation of DDS ions inside the galleries of LDH. This increase in d-spacing from about 0.76 to 2.57 nm indicates the perpendicular monolayer arrangement of DDS ions in the LDH galleries.[15]

The presence of DDS ions in the MLDH galleries was also confirmed by FTIR (Figure 3). The broad peak in the range 3900–3100 cm^{-1}, centered at 3500 cm^{-1} is due to the O—H stretching vibrations of the surface and interlayer water molecules. The bending vibration of water molecules observed at 1630 cm^{-1}. The bands at 2850, 2920, and 2956 cm^{-1} are because of —CH_2 and —CH_3 in aliphatic chains of dodecyl sulfate. A strong absorption band at 1215 cm^{-1} is assigned to the stretching vibrations of a sulfate group while a band at 1469 cm^{-1} is due to the presence of methylene group.

Figure 4 display the electron micrographs of the LDH and MLDH. The micrographs were obtained using SEM at 2000× magnifications. Figure 4(a) shows a typical hexagonal platelet structure characteristic for LDH particles obtained for MgAl-Cl LDH. The regularity of the LDH particles confirmed the fine crystallinity as evidenced by X-ray measurement. The thickness of these platelet-stacks is around few hundred nanometers and the lateral dimension is in the range of 1–2 μm. In case of MgAl-SDS (MLDH) [Figure 4(b)], the morphological features seem quite similar that to parent LDH and gives evidence for retention of hexagonal platelet LDH morphology. However, the shape of the particles seems slightly irregular and stacked in comparison to the unmodified LDH. This was probably due to the hydrophobic interaction of the LDH surface-adsorbed SDS particles. The size and interlayer arrangements of surfactant anions may be a potential factor that influences stacking and growth of the metal hydroxide layers during the regeneration process. Overall, it can be said that such methods not only regenerates the metal hydroxide sheets but also the plate-like geometry of the primary particles. Conclusively, the nanohybrid structure of LDH was confirmed by SEM.

Electrospun Fiber Morphology

The electrospun fiber morphology of PVDF and PVDF/MLDH nanocomposites was shown in Figure 5. It is clearly seen from the micrograph that pristine PVDF exhibited nonuniform fibers with the size ranging from 80 to 600 nm. A large number of beads of about 3–5 μm were also seen. However, for PVDF/MLDH nanocomposites, the nanofibers with size ranging from

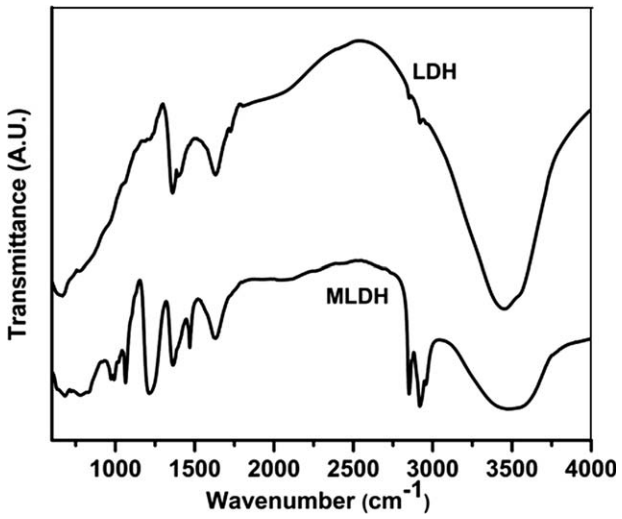

Figure 3. FTIR micrograph for LDH and MLDH.

Applied Polymer SCIENCE

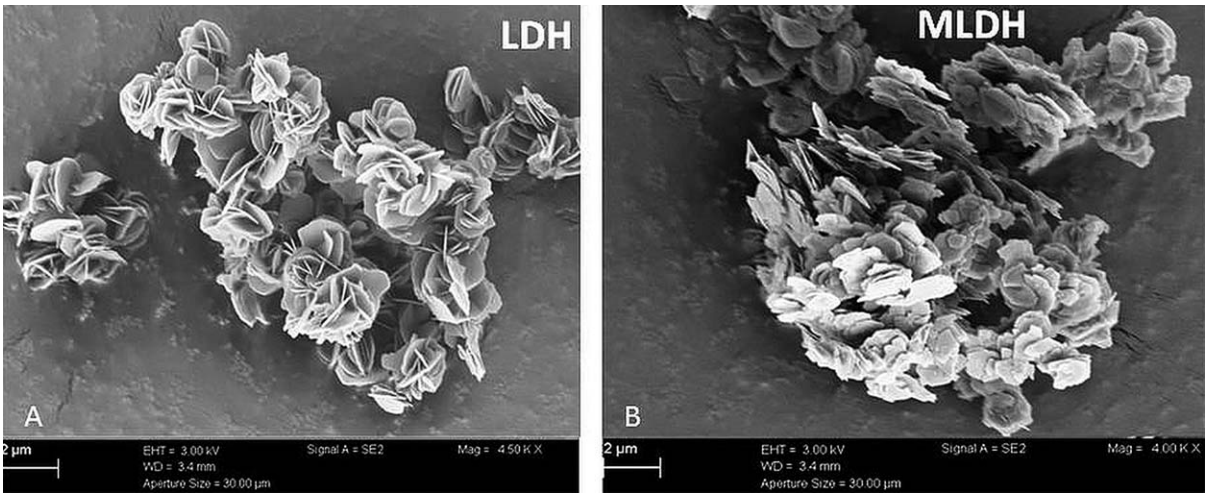

Figure 4. Scanning electron micrograph of LDH (A) and MLDH (B).

80 to 200 nm were observed. It is also to be noted that these fibers are almost bead free. As the concentration of MLDH increased to 10 wt %, nanofibers with a slightly rough surface were obtained. It is clear from the figure that the rough surface is due to nanoscale aggregation of the MLDH particles. The morphology and diameter of electrospun fibers depend on various parameters like, strength of applied electric field, feeding rate (processing properties), viscosity, conformation of polymer chains, elasticity, surface tension, and polarity of the solvent, and electrical conductivity of the polymer solution (solution

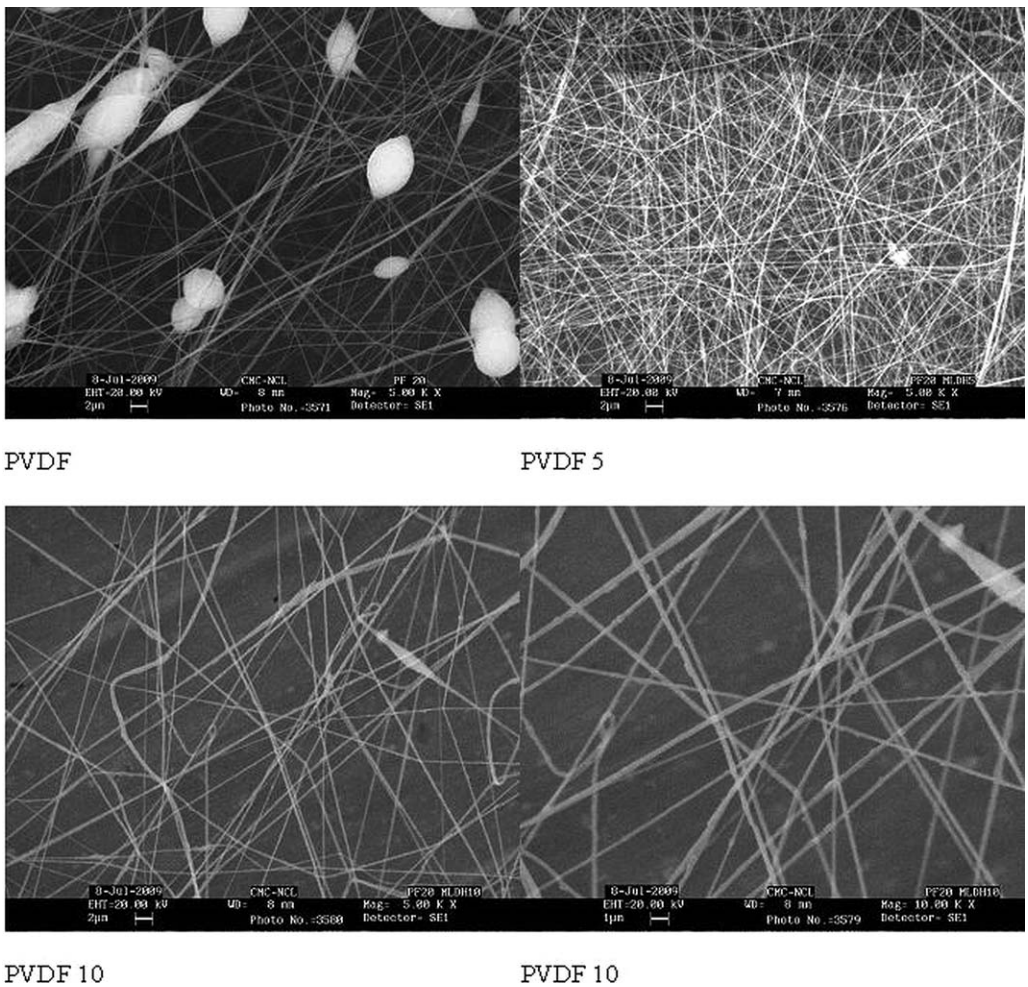

Figure 5. Fiber morphology of PVDF and PVDF/MLDH nanocomposites.

Table I. Conductivity and Viscosity of PVDF and PVDF/MLDH Nanocomposites

Sample	Conductivity (μS/cm)	Viscosity (cPs) @ 0.5 rpm
PVDF	2.43	290
PVDF 5	48.9	530
PVDF 10	51.3	2560

properties). It is important to note that the addition of MLDH to PVDF solution enhances the conductivity due to the presence of charges on LDH and DDS ions also the viscosity was found to be increased because of dispersion of MLDH.

According to the literature,[17] viscosity and conductivity play an important role on the morphology and the diameter of electrospun nanofibers. It has been reported that increase in viscosity resulted in increase in fiber diameter, while for conductivity, it is vice a versa. It is known that the charged ions present in the polymer solution have significant influence on the jet formation. In the processes of electrospinning, the ionic solutions develop, increased charge to charge repulsion as the ionic concentration increases, hence, produces higher tension leading to the formation of Taylor cone, due to which fine and uniform nanofibers are formed. According to Table I, the viscosity and the conductivity of the PVDF/MLDH solutions were found to be increased. Therefore, we can say that the conductivity dominates over viscosity contributions in determining the morphology of the electrospun fibers. Thus the reinforcement of MLDH to the PVDF produces uniform, smaller and bead free nanofibers; this can be attributed to the enhanced conductivity of PVDF solution.

Structure Evaluation

The microstructure of the electrospun PVDF/MLDH nanocomposite nanofibers was evaluated using X-ray diffraction. Figure 6 depicts the X-ray diffraction patterns for MLDH and PVDF/MLDH nanocomposites. As described earlier, the basal peak position for MLDH was found to be at 2 theta of 3.04°, whereas in nanocomposites, this peak was completely absent. The absence of peak does not mean always an exfoliated structure, as the absence of peak may be due to loss of coherent scattering or random orientation of MLDH layers. The other reason is due to intercalation of polymer chains inside the galleries of MLDH; the gallery spacing might have increased more than 4 nm that cannot be measured (2 - theta angle <2°) due to the limitation of XRD instrument. Thus the nanocomposite nanofibers exhibit delaminated and/or exfoliated structure.

Polymorphism in Electrospun Nanofibers

The X-ray diffraction patterns for electrospun mats of PVDF and PVDF/MLDH nanocomposite were shown in Figure 6. PVDF electrospun mat exhibit diffraction peaks at 2 theta of 18.7, 20.6, and 27.1° which correspond to 020 (α), 200/110 (β), and 111/021 (α) planes, respectively. Presence of these diffraction peaks suggests that α and β crystal phases coexist in PVDF fibers. Basically, in the electrospinning process, two types of forces are exerted on a polymer solution, one is shear force when it flows through the needle and the second is Coulombic force when the jet is elongated and accelerated by the high electric field applied. This stretching of polymer chains while electrospinning can facilitate the transformation of α phase into β phase. The PVDF/MLDH nanocomposites exhibited same diffraction patterns. However, the intensity of peaks such as 18.7 and 27.1° corresponding to α crystalline form was found to be reduced. The peaks at 18.7 and 27.1° almost diminished suggesting that the content of α crystalline phase decreased as the concentration of MLDH increased.

The electrospun mats were characterized by FTIR to confirm the presence of β crystalline phase in PVDF. Figure 7 shows FTIR transmittance for electrospun PVDF and PVDF/MLDH nanocomposites. The bands at 615, 765, and 976 cm^{-1} confirm the presence of α phase which exhibit TGTG' conformations. The band at 615 cm^{-1} is assigned to mixed mode of CF_2 bending and C—C—C skeletal vibration and is parallel to chain axis. The transmittance band at 765 cm^{-1} is related to rocking vibrations.

Figure 7 also demonstrates that the FTIR transmittance for the bands at 765 and 976 cm^{-1} has been significantly reduced, suggesting that the presence of MLDH impedes the TGTG' conformations of PVDF. If the polymer chains have longer transsequences than TT, the bands at 840 and 1274 cm^{-1} appears. These bands are characteristic of β-crystalline phase of PVDF, which have TTTT conformations.[18] The band 840 cm^{-1} is assigned to mixed mode of CH_2 rocking and CF_2 asymmetric stretching vibrations and this mode is parallel to chain axis. From figure, it can be clearly understood that the intensity of the transmission bands at 840 and 1274 cm^{-1} has been increased. From these results, it is evident that the introduction of MLDH in PVDF matrix induces more β crystalline phase.

The symmetric and asymmetric stretching vibrations of —CH_2 groups show the transmission bands at 2980 and 3020 cm^{-1}

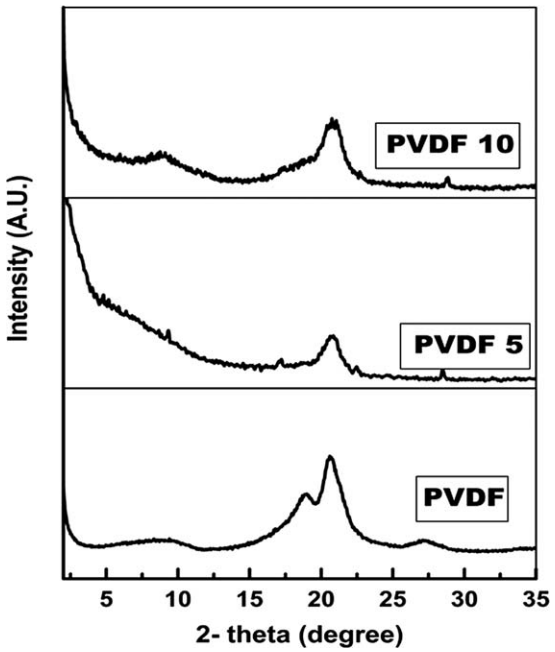

Figure 6. X-ray diffraction pattern for PVDF and PVDF/MLDH nanocomposites.

Applied Polymer SCIENCE

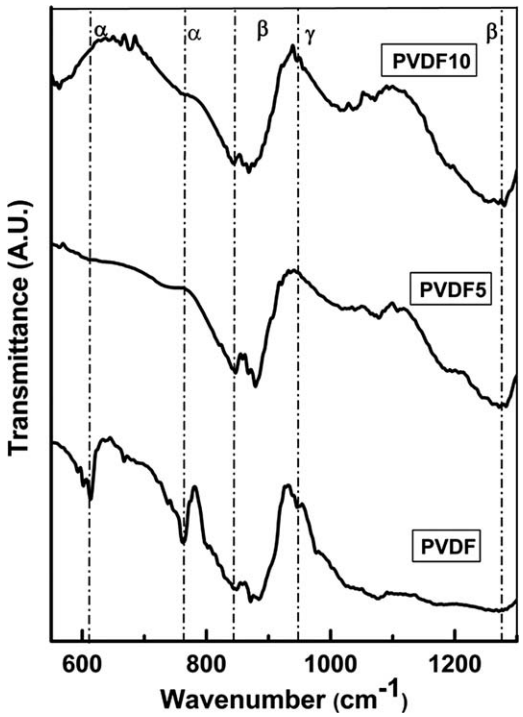

Figure 7. FTIR micrograph for PVDF and PVDF/MLDH nanocomposites.

(Figure 8).[19] The symmetric vibrations are generally weaker than asymmetric vibrations. The —CH_2 stretching bands occur due to the PVDF monomer. However, these two bands systematically decreased with the content of MLDH, which suggests that the presence of MLDH impedes the stretching vibrations due to strong interactions.

The introduction of nanofiller to the polymer matrix which exhibit polymorphism revealed a significant effect on the type of crystalline phases formed. From the above discussion, it can

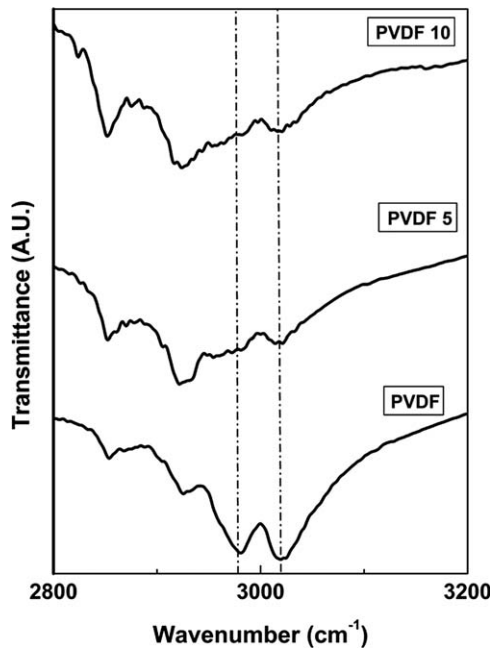

Figure 8. Symmetric and asymmetric stretching vibrations of –CH_2.

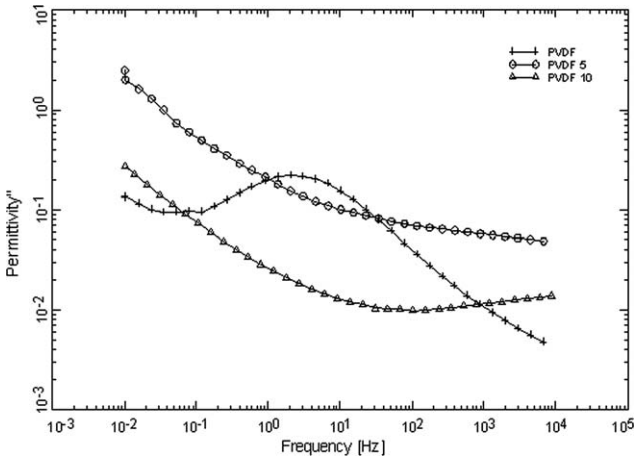

Figure 9. Dielectric relaxations in PVDF and PVDF/MLDH nanocomposite.

be concluded that the addition of MLDH effectively improved the electrospinnability, morphology, and β phase content of PVDF. Yee et al.[5] studied the system in which the presence of salts enhanced the β crystalline phase in PVDF.

This enhancement in β phase of PVDF can be explained on the basis of presence of interlayer water molecules in MLDH, which leads to hydrogen bonding between water molecules and the fluorine atoms of PVDF.[20]

Dielectric Properties

The dielectric loss (ε'') in the range of 10^4-10^{-2} Hz for pristine PVDF and the nanocomposites is shown in Figure 9. A comparison of the curves of ε'' for pristine PVDF and the nanocomposites shows clearly the effect of reinforcement of MLDH. The relaxation observed at around 1 Hz for pristine PVDF is due to the relaxation in the crystalline α phase. Interestingly, this relaxation was not observed in the case of nanocomposites. However, it is reported that β phase PVDF does not show any relaxation in this particular range of frequencies.[21] Thus, the dielectric analysis also confirms the presence of the β phase of PVDF in the nanocomposites.

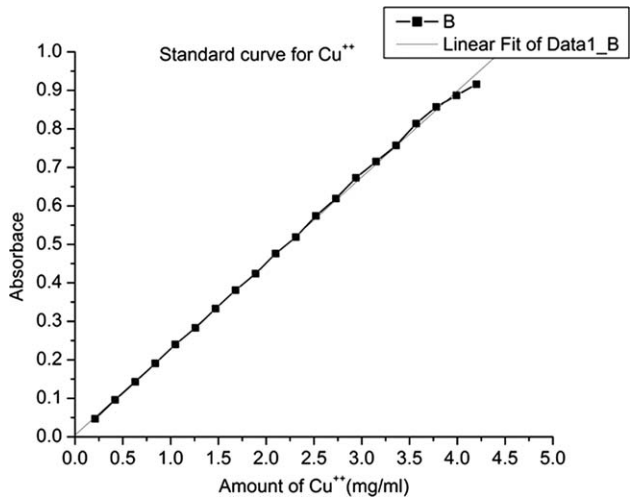

Figure 10. Standard calibration curve of the metal salt.

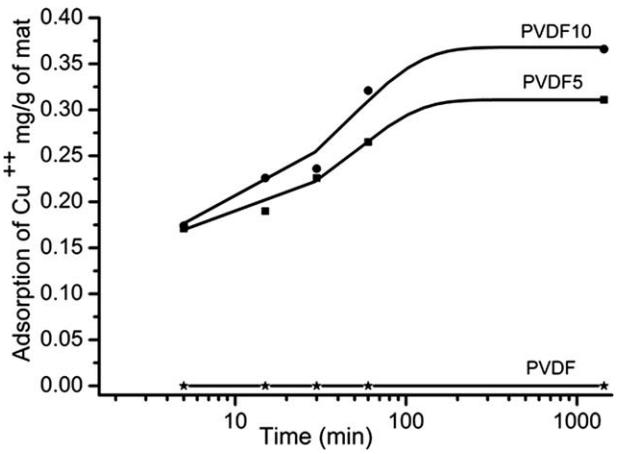

Figure 11. Adsorption capacity of Cu (II) of PVDF and PVDF/MLDH.

Metal Ion Adsorption Studies

As discussed in the introductory part, LDH is being used in separation technology. The electrospun mats of PVDF with LDH are first time used for metal ions removal from water. The detailed discussion of this study has been explained. In this study, a 5 mg of the respective nanofiber mats of PVDF with and without MLDH were transferred in 3 mL of 2% $CuSO_4$ solution. The nanofiber mats were removed at various time intervals from the solution, filtered, and the optical density of the respective metal solution was evaluated by UV–visible spectrophotometer [UV-1601(PC) S, Schimadzu, Japan] at the respective λ_{max} of the standard solutions. Known standard solutions, such as, copper sulfate ($\lambda_{max} = 780$), was used for determining the metal concentrations. The exact amount of metal adsorbed by the material was calculated from the respective calibration curve (Figure 10) of the metal salts. The studies were repeated twice for reproducibility.

The absorbance of copper sulfate was found to decrease with time. The decrease in absorbance was comparatively very fast in the beginning; after 12 h, it remains almost constant. From the absorbance, the concentration of Cu (II) ion was determined and the adsorption capacity of the nanofiber mat was calculated. EDAX was used to confirm the presence of Cu (II) ions and to measure its quantity adsorbed on the nanofibers mats. Both UV–vis spectroscopy and the EDAX revealed

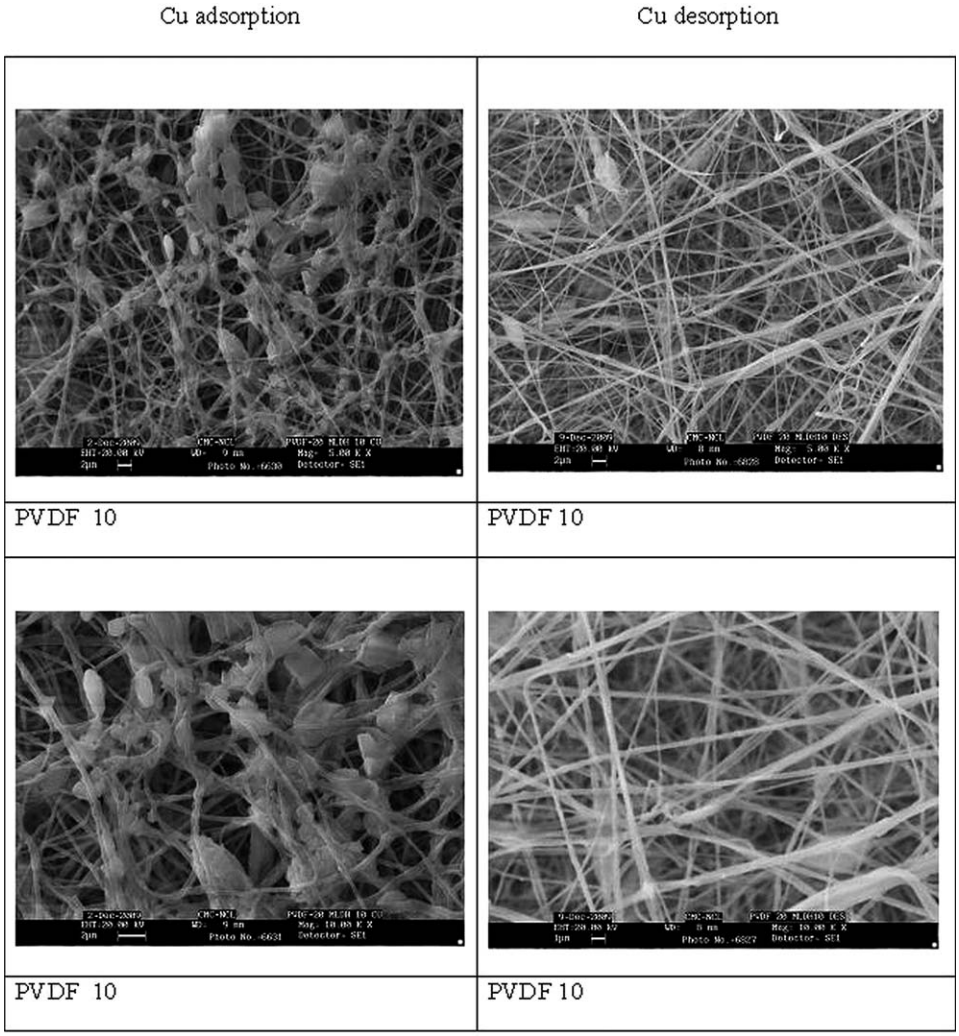

Figure 12. Scanning electron micrographs for Cu (II) adsorption and desorption.

almost the same concentration of adsorbed Cu (II) ions. The adsorbed concentration of Cu (II) in nanocomposite mat is shown in Figure 11. It is clear from the figure that as the concentration of MLDH increased, the adsorption capacity was found to increase, suggesting that the MLDH have very good capacity for adsorption of metal ions. The sorption mainly occurs as anion exchange and surface adsorption in LDH.[22] As discussed in an earlier section, MLDH is found to be exfoliated due to intrusion of PVDF molecular chains in the galleries. Also MLDH have hydroxide layer in their structure so the surface adsorption is found to be the significant mechanism for the metal ion adsorption. This is also confirmed from the SEM micrographs of the nanofiber mats. From Figure 12, it is clearly evident that the surface adsorption is dominant as the $CuSO_4.5H_2O$ is found to be physically sorbed on the fibers surface. It is important to note that there was no significant change in the morphological structure of the nanofibers of PVDF/MLDH after soaking in the $CuSO_4.5H_2O$ solution for 24 h.

The re-usability of these nanofiber mats was also examined. The above mats which have been used for metal ion adsorption studies were again kept in de-ionized water for 24 h to quantify the desorbed amount of Cu (II) ions in the de-ionized water. From SEM micrographs (Figure 12) and the EDAX analysis, it is concluded that the mats can be re-used for metal adsorption.

CONCLUSIONS

PVDF/MLDH nanofiber mats were prepared successfully using electrospinning. The nanofiber morphology of PVDF could be tailored effectively by introducing MLDH. The enhancement in conductivity of the solution resulted in significant reduction in the number and size of the beads and the diameter size distribution of the nanofibers. The X-ray diffraction patterns portrayed an exfoliated structure for the nanocomposites. It also can be revealed from the X-ray diffraction patterns that the pristine PVDF mainly exhibited α and β phases and small amount of γ phase. However, introduction of MLDH resulted in predominant β phase and decrease in α phase of PVDF. The dielectric analyses, which exhibited no relaxation in the frequency ranges from 10^{-1} to 10^3 Hz, also support the formation of β phase. This enhancement of the β phase content of PVDF was attributed to the possible interactions between water molecules and fluorine atoms that lead to hydrogen bonding. In an application point of view, these nanofiber mats were found to be effective in removal of heavy metal ions such as Cu (II) from water.

ACKNOWLEDGEMENT

S.D.W. and S.P.L. thank CSIR, New Delhi, India for financial assistance. The authors also thank A.B. Gaikwad for SEM and J. P. Jog for valuable comments

REFERENCES

1. Lovinger, A. J. Polyvinylidene Fluoride. In: Developments in Crystalline Polymers; Bassett DC., Ed.; Applied Science: London, **1982**; Vol. I Chapter 5, pp. 195-261.
2. Hasegawa, R.; Kobayashi, M.; Takodoro, H. *Polym. J.* **1972**, *3*, 591.
3. Nandi, A. K.; Mandelkern, L. *J. Polym. Sci. Part B: Polym. Phys.* **1991**, *29*, 1287.
4. Prest, W. M.; Luca, D. J. *J. Appl. Phys.* **1975**, *46*, 4136.
5. Yee, W.; Kotaki, M.; Liu, Y.; Lu, X. *Polym.* **2007**, *48*, 512.
6. Mago, G.; Kalyon, D.; Fisher, F. *J. Nanomate.* **2008** Article No. 759825.
7. Priya, L.; Jog, J. *J. Polym. Sci. Part B: Polym. Phys.* **2002**, *41*, 31.
8. Asai, K.; Okamoto, M.; Tashiro, K. *Polymers* **2008**, *49*, 4298.
9. Gregorio, R. *J. Appl. Polym. Sci.* **2006**, *100*, 3272.
10. Andrew, J.; Clarke, D. *Langmuir* **2008**, *24*, 8435.
11. Zheng, J.; He, A.; Li, J.; Han, C. C. *Macromol. Rapid Commun.* **2007**, *28*, 2159.
12. Yu, L.; Cebe, P. *Polym.* **2009**, *50*, 2133.
13. Liu, Y.; Li, Y.; Xu, J.; Fan, Z. *ACS Appl. Mater. Interface* **2010**, *2*, 1759.
14. Costa, F.; Grenzer, M.; Wagenknecht, U.; Heinrich, G. *Adv. Polym. Sci.* **2008**, *210*, 101.
15. Newman, S.; Jones, W. *New J. Chem.* **1998**, *22*, 105.
16. Hamzah, Z.; Rahman, M.; Yasin, Y.; Sumari, S.; Saat A. *J. Nucl. Rel. Tech.* **2011**, *8*, 60.
17. Pham, Q.; Sharma, U.; Mikos, A. *Tissue Eng.* **2006**, *12*, 1197.
18. Ramasundaram, S.; Yoon, S.; Kim, K.; Park, C. *J. Polym. Sci. Part B: Polym. Phys.* **2008**, *46*, 2173.
19. Lanceros-Mendez, S.; Mano, J.; Costa, A.; Schmidt, V. *J. Macro. Sci. Part B* **2001**, *40*, 517.
20. Benz, M.; Euler, W. B.; Gregory, O. J. *Macromolecules*, **2002**, *35*, 2682.
21. Oka, Y.; Koizumi, N. *Polym. J.* **1982**, *14*, 869.
22. Nedim, A. Ay.; Zumreoglu-Karan, B.; Temel, A. *Microp. Mesop. Mate.* **2007**, *98*, 1.